ChemComm

Accepted Manuscript

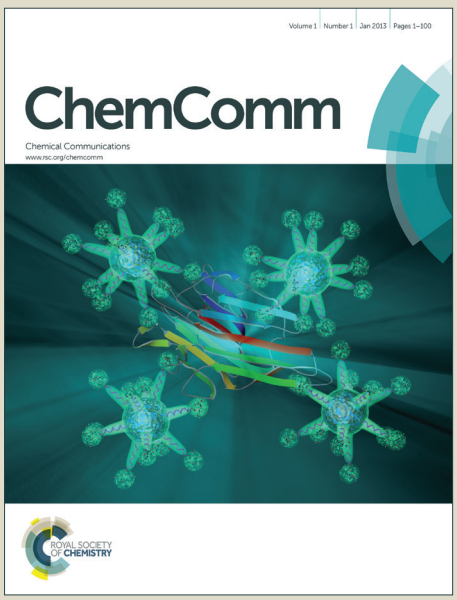

ROYAL SOCIETY OF CHEMISTRY

www.rsc.org/chemcomm

ChemComm

Cite this: DOI: 10.1039/c0xx00000x

www.rsc.org/chemcomm

COMMUNICATION

The photocathodic properties of $Pb(Zr_{0.2}Ti_{0.8})O_3$ wrapped $CaFe_2O_4$ layer on ITO coated quartz for water splitting

Xiaorong Cheng, Deliang Chen, Wen Dong, Fengang Zheng, Liang Fang and Mingrong Shen*

Received (in XXX, XXX) Xth XXXXXXXXX 200X, Accepted Xth XXXXXXXXX 200X

DOI: 10.1039/b000000x/

$Pb(Zr_{0.2}Ti_{0.8})O_3$ wrapped $CaFe_2O_4$ particle structure were constructed on ITO coated quartz as a photocathode for efficient water splitting. A photocurrent of 152 μA cm^{-2} was obtained under zero bias *vs.* Ag/AgCl and 100 mW cm^{-2} with the assistance of positively poling and Ag decoration.

Since Fujishima *et al.* reported the n-type TiO_2 as photocatalyst for water splitting,[1] photoelectrodes based on semiconductor materials have been extensively studied. Metal oxides with a narrow band gap such as WO_3,[2] Fe_2O_3,[3] $BiVO_4$,[4] and TaON,[5] have attracted much attention for their low cost, visible light activity and stability in electrolyte. However, they are mostly n-type and studied as photoanodes. Researches on metal oxide photocathodes are quite small. Examples of the latter include Cu_2O, Rh doped $SrTiO_3$, and $CaFe_2O_4$ (CFO).[6-8] Still, these materials do not provide the stability combined with good spectral photoresponse and high energy conversion efficiency needed for practical water splitting. P-type CFO with a band gap of 1.9 eV may be a good potential photocathode material. Ida *et al.* reported a CFO photocathode prepared on Pt substrate having a short circuit photocurrent of 200 μA cm^{-2} under 500 W Xe lamp illumination when connecting with a n-type TiO_2 electrode.[8] Unfortunately, this CFO electrode was prepared at a high annealing temperature of 1200°C, making it impossible be prepared on most transparent conduction substrates like ITO/glass.

The ferroelectric films with spontaneous and reversible polarization, such as $Pb(Zr,Ti)O_3$,[9] $BiFeO_3$,[10] and $BiFeCrO_6$,[11] have been intensively studied as potential photovoltaic materials in recent years, where the depolarization field (E_{pi}) originating from the electric polarization that exists throughout the whole film and the barriers on film/electrode interface dominate the photovoltaic properties.[12,13] Our recent studies revealed that the $Pb(Zr_{0.2}Ti_{0.8})O_3$ (PZT) film fabricated on ITO/quartz can be worked as a photocathode in aqueous electrolyte.[14] However, PZT films can only absorb UV light. Combining the PZT films with narrow band gap semiconductor is supposed to be an efficient way to encompass the UV to visible light spectra and enhance the photovoltaic efficiency of PZT films.[15] In this study, we try to combine PZT and CFO to form a photocathode on ITO coated quartz. CFO is used to absorb visible light and PZT to absorb UV light and separate the photogenerated carriers by remnant depolarization field. A thin PZT layer was firstly crystallized on ITO/quartz to ensure a close contact between ITO and PZT, and subsequently an amorphous PZT (a-PZT) layer was deposited on PZT/ITO. CFO particles were firstly prepared through ordinary calcination method under high temperature of 1050°C, and then deposited on a-PZT/PZT/ITO by electrophoretic deposition (EPD). The loose CFO particles were then wrapped intimately by spin-coating another PZT layer on the top. At last, the whole a-PZT/CFO/a-PZT/PZT layer was sintered under 650°C. We called such layer as PZT/CFO/PZT (PCP) layer. Ag particles deposited on the film surface by photochemical reduction were used to enhance the photoelectrochemical (PEC) properties. The experimental details were presented in the ESI.†

Fig. 1a shows the loosely stacked CFO particles deposited by EPD method on PZT/ITO. This is reasonable since the particles is attracted each other only by electrical field in this stage, and annealing under 650°C is not sufficient to re-crystallized the CFO layer which can not be well crystallized below 1000°C. In addition, the CFO layer is porous resulting from the irregular particle sizes of CFO powders. This CFO layer is also loosely contacted on the PZT/ITO/quartz substrate, as demonstrated in Fig. 1b. An obvious gap can be seen between them. The poor connection among CFO and between CFO and substrate leads to the poor photocurrent of about 1.5 μA cm^{-2} (Fig. S1, ESI†). We also found that the one have bottom or top PZT layer also exhibits quite low photocurrent, because the former has poor connection among CFO and the latter has poor connection between CFO and substrate (Fig. S2, ESI†).

The surface morphology of PCP film is shown in Fig. 1c and 1d. The interparticle connection happens due to the PZT gel penetrating from the top of the CFO layer, which fills the void between CFO particles. A close contact between the CFO layer and substrate can also be observed in Fig. 1d. EDX analysis for the cross section of the PCP layer is performed and presented in support information (Fig. S3, ESI†). The PZT elements are dispersed all through the PCP film, not only existing on the bottom and top of the layer. This means that PZT wraps the CFO particles in the whole layer (Fig. S4, ESI†). The CFO powder is well crystallized and represents an orthorhombic structure which is in accord with references,[16,17] and the PZT XRD pattern has a polycrystalline perovskite structure (JCPDS card No. 70-4260). The XRD pattern of Ag in PCP film represents pure Ag crystal

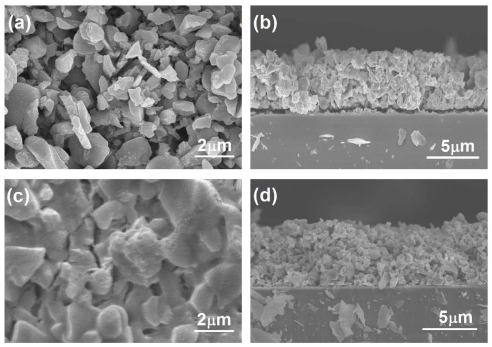

Fig. 1 The SEM surface (a) and cross-section (b) of the CFO layer deposited on PZT/ITO by EPD method. (c) and (d) are the corresponding ones for the PCP layer.

phase (JCPDS card NO. 65-2871) which confirms that Ag nanoparticles is formed on the PCP film surface by photoreduction (Fig. S5, ESI†).

As discussed above, the CFO layer without the bottom and top PZT coatings exhibits a very low photocurrent of about 1.5 μA cm^{-2}. In contrast, the PCP film demonstrates a significant enhancement in the photocurrent to about 40 μA cm^{-2}, indicating that the PZT wrapped structure is crucial to the separation and transport of light induced electron-hole pairs. When the PCP film was polarized by a positive applied voltage to the film versus the reference electrode, E_{pi} is enhanced across the PZT with the direction pointing from layer/electrolyte interface to ITO. In this case, the cathodic photocurrent of PCP film increases to 80 μA cm^{-2}, since E_{pi} is beneficial for the separation of photogenerated carriers. As expected, it decreases to about 5 μA cm^{-2} if the sample is poled by a reverse electric field. The photocurrent can be further enhanced to about 152 μA cm^{-2} after the Ag is decorated on the film surface, as Ag decoration on the PZT surface can enhance the visible light utility and form a favorable energy level alignment for efficient electron-extraction and thus modify the film/electrolyte contact.[14] Note there is an optimal deposition time for the photoreduction of Ag^{+} (Fig. S6, ESI†).

In Fig. 2b, we also compare the current–voltage behavior of the as-prepared PCP film with the positively poled and positively poled plus Ag decorated ones. The zero-current potentials for the three samples are 0.21, 0.35 and 0.44 V *vs.* Ag/AgCl, respectively. Thus, both the positive poling and the Ag decoration make the open-circuit voltage of the photocathode enhance significantly, consistent with the enhancement of the photocurrent. Based on the current–voltage curve, the solar-to-chemical conversion efficiency for the positive poled and Ag decorated PCP film is determined to be nearly 0.1% (Fig. S7, ESI†).

To understand the increment of photocurrent, we measured in Fig. 3a the UV-vis diffused reflection spectra (DRS) of the PZT film, CFO and PCP layers, respectively. The absorption of CFO has a clear edge around 650 nm, which corresponds to the band gap of CFO.[17] The absorption edge around 400 nm of PZT film on ITO quartz comes from the band gap of PZT. The absorption of PCP film has both two clear edges of CFO and PZT. This implies that the light-harvesting of PCP film is due to the narrow band of CFO and broad band of PZT that encompass the UV to visible light spectra, which converts into the photocurrent (Fig.

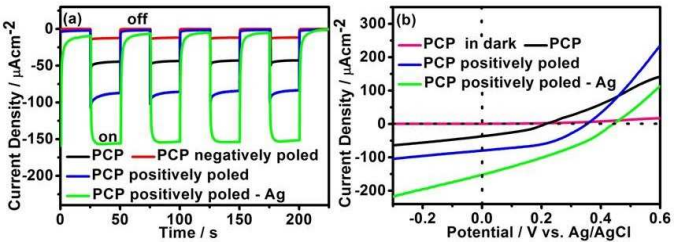

Fig. 2 (a) Photocurrent under zero voltage *vs.* Ag/AgCl measured in a PEC cell using 0.1 M Na_2SO_4 solution as electrolyte and 100 mW cm^{-2} illumination for the as-prepared (black) PCP film, positively (blue) or negatively (red) poled PCP film, and positively poled and Ag decorated (green) PCP film. (b) Current–voltage curves of samples shown in (a) except the negatively poled one. The one for the as-prepared PCP film in dark is shown as pink, which is close to zero.

S8, ESI†). Based on the absorption spectra, we measured the photocurrent using a wavelength cutoff filter of 420 nm in order to separate the contribution from the visible light where PZT does not excited. Fig. 3b shows that the photocurrent coming from the visible light (> 420 nm) for the as-prepared PCP film is 22 μA cm^{-2}. When the film is positively poled, the visible light photocurrent increases significantly to 50 μA cm^{-2}, implying that E_{pi} not only helps to separate the photocarriers generated in PZT, but also the ones generated in CFO. For the case of Ag decorated on the as-prepared PCP films, the visible light photocurrent also increases obviously to 50 μA cm^{-2}, manifesting that Ag nanoparticles contacted on the PZT surface enhance the visible light utility, consistent with our previous study.[14] When Ag is decorated on the polarized PCP film, the visible light photocurrent enhances to 120 μA cm^{-2}. Clearly, the two factors, E_{pi} and Ag decoration are both important for the enhancement of photocurrent observed in Fig. 2a.

The corresponding EIS measurement was also carried out at the same condition as the photocurrent measurement. In Fig. 3c the samples show pronounced arcs at higher frequencies, whose diameters manifest the reaction rate occurring at the surface of electrode.[18] Based on the Nyquist plots, significant changes in the EIS are observed. Comparing with the as-prepared sample, the semicircle decreases significantly as the PCP film is positively polarized or decorated by Ag, indicating a more effective separation of photo-generated electron/hole pairs and fast charge transfer to the electron donor/electron acceptor on the film surface.[19] The polarized plus Ag decorated PCP film shows the smallest semicircle, illustrating the best for the charge separation and transfer, consistent with the observed enhanced PEC properties shown in Fig. 2 and Fig. 3b.

According to the analysis in S5 and S9 of ESI†, we proposed that the PZT wrapped CFO structure may contribute mainly to the visible-light photocurrent. A physical picture is therefore described in Fig. 3d to explain the point, where the energy band structure of a symmetrical PZT/CFO/PZT heterojunction is sketched. The built-in electric fields induced at the left and right PZT-CFO junctions have the same magnitude but opposite direction if there are no other internal electric field in the film. They do not contribute to separation and transport of the photocarriers. However, the PZT film may be self-polarized, and

also there is an interface barrier on ITO/PZT.[13] This leads to the photocathodic current of the as- prepared film. If the film is

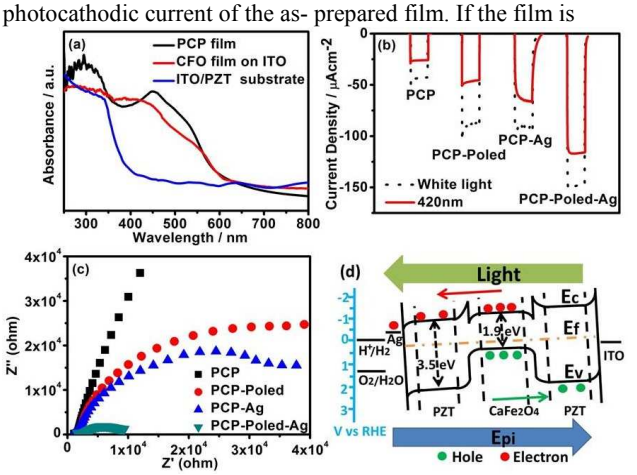

Fig. 3 (a) The UV-vis DRS spectra of PZT, CFO layer deposited by EPD and PCP film; (b) Photocurrent density (solid lines) of different PCP films with wavelength cutoff filter of 420 nm and 0.1 M Na_2SO_4 solution as electrolyte. The dotted lines are those measured without the filter; (c) EIS spectra of the different samples; (d) The energy band structure of the positively poled and Ag decorated PCP film.

positively poled, the electric field E_{pi} in the bulk region of a polarized PZT thin film modifies the potential of each energy level (i.e. E_c, E_v and E_f), and provides a more strong driving force to drive the photocarriers out from the CFO,[20] resulting in the obvious photocurrent in polarized sample when high energy photons(λ<420 nm) are filtered out.

The evolution of hydrogen gas during the water splitting reaction under illumination was measured and the photocurrent during the reaction was also recorded by electrochemical workstation to calculate the amount of electrons passing through the outer circuit. Fig. 4 shows a time course of hydrogen evolution from the PCP film (cathode)-Pt (anode) electrode system in H_2 saturated acidic 1M $HClO_4$ solution under zero voltage *vs.* Ag/AgCl. During the measurement, bubbles can be seen on the surface of PCP film and Pt mesh. The amount of H_2 evolved is less than half of the electrons passing through the outer circuit. The Faradic efficiency for the H_2 production reached nearly 80% in the first 20 minutes. Then, gas production rate decreased with increasing irradiation time. After 2 hours, the Faradic efficiency for the H_2 production decreased to nearly 60%. The efficiency of H_2 evolution was less than 100% and decreased with increasing irradiation, probably due to the unwanted backward reaction between H_2 and O_2.[17] In addition, the stability issues of the photoelectrode may also cause the reduction of efficiency with time although the corrosion of electrode surface is not so evident (Fig. S9, ESI†). In spite of these limitations, the result clearly shows that the polarized PCP decorated with Ag nanoparticles can actually work as photocathode. Note the O_2 production is observed on the Pt anode (Fig. S10, ESI†).

In conclusion, we fabricated a PCP structure on ITO/quartz transparent substrates under 650°C. The photocathodic properties can be significantly improved by the composite structure, poling the ferroelectric PZT and decorating the layer/electrolyte interface by Ag. A photocurrent of 152 μA cm^{-2} was obtained under zero bias *vs.* Ag/AgCl and 100 mW cm^{-2} illumination, where 120 μA cm^{-2} is from the visible light (> 420 nm).

This work was supported by National Natural Science Foundation of China (Grant No. 91233109, 51272166) of China

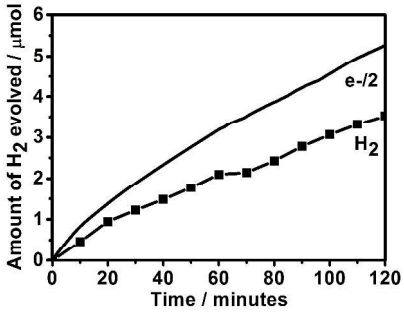

Fig. 4 Hydrogen evolution for the positively poled and Ag decorated PCP photocathode measured under 1M $HClO_4$ solution as electrolyte and 100 mW cm^{-2} illumination.

(Grant No. 91233109, 51272166), Specialized Research Fund for the Doctoral Program of Higher Education (20133201110003), and a Project Funded by the Priority Academic Program Development of Jiangsu Higher Education Institutions (PAPD).

Notes and references

Department of Physics & Jiangsu Key Laboratory of Thin Films & Collaborative Innovation Center of Suzhou Nano Science and Technology, Soochow University, Suzhou 215006, China. Email: mrshen@suda.edu.cn

† Electronic Supplementary Information (ESI) available: Experimental procedure and other informations for the PCP photoelectrodes (S1-S11). See DOI: 10.1039/b000000x/

1 A. Fujishima and K. Honda, *Nature*, 1972, **238**, 37.
2 C. Santato, M. Ulmann and J. Augustynski, *J. Phys. Chem. B*, 2001, **105**, 936.
3 D. K. Zhong, J. Sun, H. Inumaru and D. R. Gamelin, *J. Am. Chem. Soc.*, 2009, **131**, 6086.
4 D. K. Zhong, S. Chio and D. R. Gamelin, *J. Am. Chem. Soc.*, 2011, **133**, 18370.
5 R. Abe, M. Higashi and K. Domen, *J. Am. Chem. Soc.*, 2010, **132**, 11828.
6 A. Paracchino, V. Laporte, K. Sivula, M. Grätzel and E. Thimsen, *Nat. Mater.*, 2011, **10**, 456.
7 K. Iwashina and A. Kudo, *J. Am. Chem. Soc.*, 2011, **133**, 13272.
8 S. Ida, K. Yamada, T. Matsunaga, H. Hagiwara, Y. Matsumoto and T. Ishihara, *J. Am. Chem. Soc.*, 2010, **132**, 17343.
9 L. Pintilie, M. Alexe, A. Pignolet and D. Hesse, *Appl. Phys. Lett.*, 1998, **73**, 342
10 S. R. Basu, L. W. Martin, Y. H. Chu, M. Gajek, R. Ramesh, R. C. Rai, X. Xu and J. L. Musfeldt, *Appl. Phys. Lett.*, 2008, **92**, 091905.
11 R. Nechache, C. Harnagea, S. Licoccia, E. Traversa, A. Ruediger, A. Pignolet and F. Rosei, *Appl. Phys. Lett.*, 2011, **98**, 202902.
12 F. G. Zheng, J. Xu, L. Fang, M. R. Shen and X. L. Wu, *Appl. Phys. Lett.*, 2008, **93**, 172101.
13 D. W. Cao, C. Y. Wang, F. G. Zheng, W. Dong, L. Fang and M. R. Shen, *Nano Lett.*, 2012, **12**, 2803.
14 C. Y. Wang, D. W. Cao, F. G. Zheng, W. Dong, L. Fang, X. D. Su and M. R. Shen, *Chem. Commun.*, 2013, **49**, 3769.
15 X. L. Yang, X. D. Su, M. R. Shen, F. G. Zheng, Y. Xin, L. Zhang, M. C. Hua, Y. J. Chen and V. G. Harris, *Adv. Mater.*, 2012, **24**, 1202.
16 Z. F. Liu, Z. G. Zhao and M. Miyauchi, *J. Phys. Chem. C.*, 2009, **113**, 17132.
17 E. S. Kim, N. Nishimaru, G. Magesh, J. Y. Kim, J. W. Jang, H. Jun, J. Kubota, K. Domen and J. S. Lee, *J. Am. Chem. Soc.*, 2013, **135**, 5375.

18 M. Woodhouse, G. S. Herman and B. A. Parkinson, *Chem. Mater.*, 2005, **17**, 4318.
19 W. H. Leng, Z. Zhang, J. Q. Zhang and C. N. Cao, *J. Phys. Chem. B*, 2005, **109**, 15008.
20 B. K. Gan, K. Yao, S. C. Lai, P. C. Goh and Y. F. Chen, *IEEE Electron Device Lett.*, 2011, **32**, 665.